BRAIN
ORIGINAL ARTICLE

A calcium-sensitive antibody isolates soluble amyloid-β aggregates and fibrils from Alzheimer's disease brain

Andrew M. Stern,[1] Lei Liu,[1] Shanxue Jin,[1] Wen Liu,[1] Angela L. Meunier,[1] Maria Ericsson,[2] Michael B. Miller,[3] Megan Batson,[4] Tingwan Sun,[4] Sagar Kathuria,[4] David Reczek,[4] Laurent Pradier[4] and Dennis J. Selkoe[1]

Aqueously soluble oligomers of amyloid-β peptide may be the principal neurotoxic forms of amyloid-β in Alzheimer's disease, initiating downstream events that include tau hyperphosphorylation, neuritic/synaptic injury, microgliosis and neuron loss. Synthetic oligomeric amyloid-β has been studied extensively, but little is known about the biochemistry of natural oligomeric amyloid-β in human brain, even though it is more potent than simple synthetic peptides and comprises truncated and modified amyloid-β monomers. We hypothesized that monoclonal antibodies specific to neurotoxic oligomeric amyloid-β could be used to isolate it for further study.

Here we report a unique human monoclonal antibody (B24) raised against synthetic oligomeric amyloid-β that potently prevents Alzheimer's disease brain oligomeric amyloid-β-induced impairment of hippocampal long-term potentiation. B24 binds natural and synthetic oligomeric amyloid-β and a subset of amyloid plaques, but only in the presence of Ca^{2+}. The amyloid-β N terminus is required for B24 binding. Hydroxyapatite chromatography revealed that natural oligomeric amyloid-β is highly avid for Ca^{2+}. We took advantage of the reversible Ca^{2+}-dependence of B24 binding to perform non-denaturing immunoaffinity isolation of oligomeric amyloid-β from Alzheimer's disease brain-soluble extracts.

Unexpectedly, the immunopurified material contained amyloid fibrils visualized by electron microscopy and amenable to further structural characterization. B24-purified human oligomeric amyloid-β inhibited mouse hippocampal long-term potentiation. These findings identify a calcium-dependent method for purifying bioactive brain oligomeric amyloid-β, at least some of which appears fibrillar.

1 Ann Romney Center for Neurologic Diseases, Department of Neurology, Brigham and Women's Hospital, 60 Fenwood Road Rm 10002Q, Boston, MA 02115, USA
2 Harvard Medical School Electron Microscopy Facility, Goldenson Building 323, 220 Longwood Avenue, Boston, MA 02115, USA
3 Division of Neuropathology, Department of Pathology, Brigham and Women's Hospital, 75 Francis St, Boston, MA 02115, USA
4 Sanofi Corporation, 49 New York Avenue, Framingham, MA 01701, USA

Correspondence to: Dennis J. Selkoe
Ann Romney Center for Neurologic Diseases
Department of Neurology, Brigham and Women's Hospital
60 Fenwood Road Rm 10002Q
Boston, MA 02115, USA
E-mail: dselkoe@bwh.harvard.edu

Received July 12, 2021. Revised December 01, 2021. Accepted December 20, 2021. Advance access publication January 27, 2022

Keywords: amyloid; Alzheimer; calcium; antibody; synaptotoxicity

Abbreviations: aCSF = artificial CSF; CHT = ceramic hydroxyapatite; fEPSP = field excitatory postsynaptic potential; GuHCl = guanidine hydrochloride; IHF = immunohistofluorescence; LTP = long-term potentiation; oAβ = oligomeric amyloid-β; SEC = size exclusion chromatography

Introduction

Amyloid plaques, one of the two major pathologic protein aggregates in Alzheimer's disease, are composed principally of insoluble fibrillar assemblies of the amyloid-β (Aβ) peptide. However, abundant biochemical and neuropathologic evidence points to soluble oligomers of Aβ (oAβ), rather than insoluble fibrils, as the peptide's most neurotoxic form. Soluble Aβ correlates better with dementia than do plaques.[1–3] Oligomeric amyloid-β from a human Alzheimer's disease brain can induce tau hyperphosphorylation[4] and neuronal hyperexcitability,[5] and impair hippocampal long-term potentiation (LTP).[6,7]

When derived from human brain (as opposed to synthetic peptides), soluble oAβ has been operationally defined as that non-monomeric Aβ that occurs in the supernatant after ultracentrifugation of Alzheimer's disease brain that has been homogenized or soaked in an aqueous buffer. Most of this material elutes in the void volume of size-exclusion chromatography columns such as Superdex 75 or Superdex 200, and has been variously termed high molecular weight oAβ or protofibrils.[8–13] In this work, we use the term 'high molecular weight oAβ'. Little is known about human oAβ structure and biochemistry, leading some to doubt its pathologic relevance or even existence.[14] Oligomeric amyloid-β may be an intermediate in the formation of mature amyloid fibrils, with the smallest forms, including dimers and other low molecular weight assemblies, being the most toxic before aggregating into high molecular weight oAβ and ultimately fibrils.[12] Neurotoxic oAβ appears readily diffusible: soaking minced Alzheimer's disease cortex in aqueous buffer recovers only ~1/8 the total Aβ compared to homogenization and yet recovers most of the Aβ-attributable synaptotoxicity.[13] Extensive work has characterized the aggregation characteristics and biochemistry of oAβ derived from $Aβ_{40}$ and $Aβ_{42}$ synthetic monomers, including such species as amyloid derived diffusible ligands, synthetic protofibrils and others. However, mounting evidence suggests that naturally occurring oAβ differs from these synthetic preparations. Human brain-derived oAβ is orders of magnitude more neurotoxic than synthetic oAβ.[4] Recent studies have identified post-translational modifications of Aβ in human brain-derived preparations not recapitulated using synthetic peptides, including C- and N-terminal truncations[15] and even covalent isopeptide bonds between individual monomers to form neurotoxic dimers.[16] Further, three high-resolution structures of amyloid fibrils derived entirely from human brain Aβ differ from the structure of fibrils derived entirely from synthetic Aβ or even synthetic Aβ templated on human amyloid plaque cores, suggesting that the oligomers preceding their respective formation differ as well.[17,18]

A challenge in studying natural oAβ is its low concentration and the lack of tools for its purification without denaturation. Here, we developed novel anti-oAβ human monoclonal antibodies after screening for oAβ-selectivity and protection against neuritic injury induced by soluble Alzheimer's disease brain extracts on human neurons. We selected two resultant human antibodies, B24 and B28, which were evaluated to protect against Alzheimer's disease brain oAβ-induced impairment of synaptic plasticity, along with a chimeric human version of our previously described oAβ-preferring antibody 1C22.[19] We discovered a unique calcium-dependent property of B24 and showed that naturally occurring human oAβ binds avidly to calcium mineral. When we used the calcium dependence of B24 to immunopurify oAβ under non-denaturing conditions (i.e. elution with EGTA), we were surprised to observe by electron microscopy short amyloid fibrils that are amenable to further structural and biochemical analysis.

Materials and methods

Additional methods are described in the Supplementary material at *Brain* online.

Indirect enzyme-linked immunosorbent assay

Two indirect enzyme-linked immunosorbent assay (ELISA) protocols were used. For experiments comparing binding of multiple antibodies to Aβ and non-Aβ antigens as in Supplementary Fig. 2, plates were coated in 1 μg/ml antigen in PBS overnight at 4°C, blocked in PBS-T (0.05% Tween-20) with 5% milk for 2 h at room temperature, then washed four times in PBS-T. Antibodies were diluted serially in PBS-T and applied for 1 h at room temperature, then washed four times in PBS-T. Rabbit anti-mouse or goat anti-human conjugated to horseradish peroxidase diluted 1:1000 in PBS-T was added for 1 h at room temperature, then washed four times in PBS-T. 3,3′,5,5′-tetramethylbenzidine was added for 10 min and the absorbance read at 450 nm.

For experiments comparing B24 and bapineuzumab binding to aggregates of truncated synthetic Aβ as in Fig. 4, $Aβ_{1–28}$ was dissolved in 7 M guanidine hydrochloride (GuHCl) with 50 mM Tris, 5 mM EDTA, pH 8.5 at room temperature overnight and chromatographed on a Superdex 75/300 Increase column in running buffer (50 mM ammonium bicarbonate, pH 8.5). $Aβ_{11–42}$ was insoluble in 7 M GuHCl and was dissolved in DMSO without chromatography. Monomeric peptides were diluted to 20 μM in size exclusion chromatography (SEC) running buffer plus 2 mM $CaCl_2$ overnight at 37°C. Aggregates were further diluted to 1 μM, and plates were coated overnight at 4°C, then blocked in Tris-buffered saline (TBS)-T (0.05% Tween-20) with 5% BSA, 2 mM $CaCl_2$ for 2 h at room temperature, then washed three times in TBS-T. Antibodies serially diluted in dilution buffer (TBS-T with 1% BSA, 2 mM $CaCl_2$) were applied for 1 h, followed by washing three times in TBS-T. Biotinylated goat anti-human IgG (Jackson Immuno, 1:10 000) was applied for 1 h, followed by washing three times in TBS-T. Last, streptavidin-HRP (R&D Biosystems, 1:200) was applied for 45 min, followed by three washes in TBS-T and detection with Western-Ready™ enhanced luminol-based chemiluminescent (ECL) substrate Plus reagent (Biolegend). All indirect ELISA results were fitted to a four-parameter dose-response model with variable slopes (Graphpad Prism).

Soluble brain extracts

Seven Alzheimer's disease brains were used, with details presented in Supplementary Table 1. Extraction of soluble protein from frozen post-mortem brain tissue using the 'soaking' method was performed as described previously.[13] Briefly, cortical grey matter was dissected, chopped at an 0.5-mm interval on a McIlwain tissue chopper, weighed and added at 1:5 w:v to extraction buffer (25 mM Tris, 150 mM NaCl, 5 μg/ml leupeptin, 5 μg/ml aprotinin, 2 μg/ml pepstatin, 120 μg/ml pefabloc, 5 mM NaF, pH 7.2). EDTA (5 mM) or EGTA (1 mM) were added when indicated. Tissue was nutated at 4°C in 50-ml Eppendorf Protein LoBind tubes for 30 min. Tissue bits were removed by spinning for 10 min at 4°C at 2000*g* in a Fiberlite F14-14 × 50 cy rotor in a Sorvall Lynx 6000 centrifuge (Thermo Fisher). The top ∼90% of supernatant was removed and spun in a SW41Ti rotor in an Optima L90K centrifuge (Beckman Coulter) at 40 000 rpm ($RCF_{av} = 197\,000g$) for 110 min at 4°C. The top ∼90% supernatant was retained. Dialysis, as indicated, was against at least 100 volumes of TBS with two buffer exchanges over 72 h at 4°C using a 2000 molecular weight cut-off cassette. In the case of homogenates, instead of chopping, grey matter was homogenized using an IKA stirrer with Dounce homogenizer attachment for 25 strokes at 850 rpm. The crude homogenate was spun in the SW41Ti as above.

Immunoprecipitation

Protein G magnetic beads (Bio-Rad) were washed in TBS in protein low-binding 96-well plates or 1.5-ml tubes. Brain extract was diluted 4–8-fold in TBS, and 0.15–1 ml diluted extract added to 20 μl washed beads. Antibodies were included at a concentration of 16.7–20 μg/ml. Plates or tubes were agitated overnight at 4°C. Beads were washed three times in TBS. Aβ was eluted and denatured by agitating overnight in TBS containing 5 M GuHCl and 5 mM EDTA. Eluate was assayed by an Aβ monomer-preferring ELISA. Serial dilution of the brain extract before immunoprecipitation resulted in excellent dilution linearity of the ELISA (Supplementary Fig. 1). For competition immunoprecipitation (as in Fig. 4A), brain extracts were diluted 8-fold and pre-incubated with 20 μl Dynabeads MyOne Streptavidin T1 (Thermo) and 100 μg/ml non-biotinylated competitor antibody for 3 h with agitation at 4°C. Biotinylated B24 (Lightning-Link Rapid Type B, Novus Bio) was then added at 2 μg/ml overnight, followed by washing, elution/denaturation in 5 M GuHCl and performing Aβ monomer ELISAs as above.

Sandwich ELISAs

The Meso Scale Discovery (MSD) platform was used to quantify $Aβ_{42}$, tau and α-synuclein. For samples denatured with GuHCl, the sample and monomer standards were diluted so the final GuHCl concentration fell to 0.25 M. Antibody pairs were as follows: $Aβ_{42}$—m266 (3 μg/ml) capture, 21F12 (0.4 μg/ml) for detection; tau—BT2 (3 μg/ml) for capture, HT7 (0.05 μg/ml) for detection; α-synuclein—MJFR1 for capture (3 μg/ml) and biotinylated Syn-1 for detection (0.25 μg/ml). Capture antibody was added to MSD plates overnight at room temperature. Plates were blocked in 150 μl TBS-T and 5% Blocker A for 1 h shaking, then washed three times with 150 μl TBS-T. Samples and standards were applied (25 μl in TBS-T containing 1% Blocker A) in duplicate or triplicate for 1.5 h shaking, then washed three times with 150 μl TBS-T. Biotinylated detector antibody was applied (25 μl in TBS-T with 1% blocker A) for 1.5 h shaking, then washed three times with 150 μl TBS-T. Detection occurred in an MSD plate reader after 150 μl of 2× MSD read buffer. The lower limit of quantitation was defined as the lowest standard with a luminescence value at least twice the blank average, and the lower limit of detection was defined as the lowest standard with value greater than the blank average plus twice the blank standard deviation.

Biolayer interferometry

Antibodies were loaded onto ProA biosensor (Sartorius, 18-5010) to density 3.5 and 1.0 nm using an Octet RED96e (ForteBio). After equilibrium, binding to 1 μM $Aβ_{40}$ or 50 nM synthetic oAβ buffered in 10 mM HEPES, 150 mM NaCl, pH 7.4, ±1 mM $CaCl_2$ was performed using 180 s association and 180 s dissociation at 25°C. Binding affinity was fitted using a 1:1 binding model.

Immunofluorescent histochemistry

Human Alzheimer's disease cortex was embedded into Tissue-Tek OCT Compound and frozen at −80°C overnight. Before sectioning at 20–30-μm thicknesses using a cryostat (Leica), deep-frozen blocks were changed to −20°C for 2 h to soften tissue for sectioning. Cryo-sections were then mounted on MAS-GP Adhesion Microscope Slides (Matsunami) and stored at 4°C before staining. Cryo-sections were equilibrated in PBS containing 0.03% Triton X-100 (PBS-TX) for 30 min followed by blocking with 5% milk in PBS-TX for 1 h. Primary antibodies were diluted in PBS-TX and added at 4°C overnight. After a wash with PBS-TX, sections were incubated with Alexa-488 or Alexa-647 conjugated secondary antibodies for 1 h followed by PBS-TX wash. Micrographs were taken using a DMi8 Widefield microscope (Leica).

Electron microscopy

All steps were performed at room temperature. Carbon-coated grids (EMS) were glow-discharged at 25 mA for 20 s, then a 5 μl sample was adsorbed to the grid for 1–5 min. Excess liquid was removed with filter paper (Whatmann No. 1). The grid was then floated on a drop of water, blotted again and stained with 0.75% uranyl formate for 15 s. Excess stain was removed with filter paper. For immunostaining, after adsorption, samples were blocked in 1% BSA. Antibody D54D2 (Cell Signaling Technologies) was added at 1:20 in 1% BSA for 20 min, then washed three times in PBS. Protein A-gold (Cell Biology UMC Utrecht) in 1% BSA was then applied for 20 min, followed by two washes in PBS and four washes in water. Samples were then fixed and stained as above. All grids were examined on a JEOL 1200EX transmission electron microscope with an AMT 2k CCD camera.

Ceramic hydroxyapatite chromatography

A Bio-Rad Foresight II (40 μm pore size) ceramic hydroxyapatite (CHT) chromatography column was equilibrated at 4°C in running buffer (500 mM NaCl, 2.5 mM $CaCl_2$, 25 mM HEPES, pH 7.4). Then, 1 ml of brain extract was diluted in 3 ml of running buffer and injected using a 5-ml loop, collecting the flowthrough in 1.5-ml fractions with a 12.5-ml washout. The column was further washed in 1 column volume (CV) of running buffer, followed by a linear gradient over 4 CV of elution buffer containing 1.5 M potassium phosphate, pH 7.4, collecting 1.5-ml fractions. The column was then washed in 3 CV of water, followed by collecting fractions in 3 CV of buffer containing 6 M GuHCl, 50 mM sodium phosphate and 50 mM HEPES, pH 7.4.

Hippocampal slice recording

Experiments were performed as previously described.[6] Briefly, mice (1–3 months old) were anaesthetized with halothane and decapitated. Transverse acute hippocampal slices (350 µm) were cut in ice-cold oxygenated sucrose-enhanced artificial CSF (aCSF) containing 206 mM sucrose, 2 mM KCl, 2 mM $MgSO_4$, 1.25 mM NaH_2PO_4, 1 mM $CaCl_2$, 1 mM $MgCl_2$, 26 mM $NaHCO_3$ and 10 mM D-glucose, pH 7.4. Slices were incubated in aCSF that contained (in mM) 124 NaCl, 2 KCl, 2 $MgSO_4$, 1.25 NaH_2PO_4, 2.5 $CaCl_2$, 26 $NaHCO_3$, 10 D-glucose saturated with 95% O_2 and 5% CO_2 (pH 7.4), in which they recovered for at least 90 min before recording. Recordings were performed in the same solution at room temperature in a chamber submerged in aCSF. To record field excitatory postsynaptic potentials (fEPSPs) in the CA1 region of the hippocampus, test stimuli were applied at low frequency (0.05 Hz) at a stimulus intensity that elicited a fEPSP amplitude that was 40–50% of maximum, and the test responses were recorded for 10 min before the experiment was begun to ensure stability of the response. Once a stable test response was attained, 0.5 ml of Alzheimer's disease brain TBS soaking extracts were added to 9.5 ml of aCSF perfusate, and a baseline was recorded for an additional 30 min. Antibodies were added to the Alzheimer's disease brain-extract aliquots at 3–5.4 µg/ml, incubated with mixing for 30 min, and then the mixture was added to the brain slice perfusion buffer. To induce LTP, we used two protocols: (i) two consecutive trains (1 s) of stimuli at 100 Hz separated by 20 s; and (ii) theta burst stimulation involving three trains, each of four pulses delivered at 100 Hz, 10 times, with an interburst interval of 200 ms with a 20 s interval between trains. Traces were obtained by pClamp 11 and analysed using the Clampfit 11. Data analysis was as follows. The fEPSP magnitude was measured using the initial fEPSP slope and three consecutive slopes (1 min) were averaged and normalized to the mean value recorded 10 min before the conditioning stimulus. All procedures involving mice were in accordance with the animal welfare guidelines of Harvard Medical School and Brigham and Women's Hospital.

Availability of data and reagents

Raw data were generated at Brigham and Women's Hospital and at Sanofi Corporation. Derived data supporting the findings of this study are available from the corresponding author on request. Patent applications for antibodies B24 and B28 have been filed, with sequences publicly available (WO2021011673). Aliquots are available to collaborators on request.

Results

Development of novel monoclonal antibodies specific for bioactive Aβ aggregates

We sought to develop a novel panel of anti-Aβ monoclonal antibodies that could neutralize the neurotoxicity of Alzheimer's disease brain-soluble extracts as observed in a 96-well functional assay we recently developed[19] and with minimal interaction with Aβ monomer or fully aggregated fibrillar Aβ. We immunized Trianni mice, which express only human immunoglobin genes, with synthetic aggregated $Aβ_{42}$ containing a mixture of aggregated species (i.e. without purification by SEC), with the goal of using diverse Aβ antigens that could generate monoclonal antibodies to be screened for protection against bioactivity of human brain-derived oAβ. The mice were boosted 3–5 times at 2-week intervals. Hybridoma clones were first screened by indirect ELISA for binding to synthetic oAβ. Twenty-eight of the 670 clones passed this primary screen and moved to counter-screening against Aβ monomers using surface plasmon resonance and against fully formed fibrils by indirect ELISA. Four clones demonstrated acceptable synthetic oAβ selectivity and moved to functional assays, all demonstrating protection of iPSC-derived wild-type human neurons against neuritotoxicity from human brain extracts. Full data on all four clones will be presented in a separate manuscript. Two of these clones, B24 and B28, are the subject of this study. The screens and counter-screens for these antibodies are presented in Supplementary Figs 2 and 3.

B24 and B28 exhibited strong binding to synthetic oAβ by indirect ELISA but no binding to Aβ fibrils or non-Aβ protein aggregates (SOD and α-synuclein) (Supplementary Fig. 2). These characteristics were comparable to our previously published oAβ-preferring mouse mAb 1C22.[19–21] For comparison, we also included 3D6, a mouse mAb that recognizes the human Aβ N terminus independent of Aβ aggregation state, and its human equivalent, bapineuzumab. Surface plasmon resonance showed that B24 did not bind to Aβ monomer, whereas bapineuzumab bound monomeric Aβ with rapid on-rate and slow off-rate (Supplementary Fig. 3). h1C22 displayed equivalent on-rate to fibrils to bapineuzumab but a more rapid off-rate (Supplementary Fig. 3), consistent with its dependence on bivalence for affinity.[19]

B24, B28, h1C22 and bapineuzumab prevent Alzheimer's disease brain-extract-induced impairment of LTP

Having originally screened our new antibodies for protection against Alzheimer's disease brain-extract-mediated disruption of neurite morphology, we verified their neuroprotective properties on inhibition of synaptic plasticity. Alzheimer's disease brain extracts can impair wild-type mouse hippocampal LTP via oAβ-dependent interference with glutamate reuptake.[6] We evaluated the ability of our new antibodies having oAβ selectivity to rescue this effect. We used Alzheimer's disease brain extracts prepared using the recently described minced cortex soaking protocol,[13] which avoids tissue homogenization (i.e. amyloid plaque breakup) to yield an aqueous brain extract enriched in highly diffusible, bioactive forms of oAβ.[13] Addition of Alzheimer's disease soaking brain extract (see Methods section) at 5% v:v to the aCSF slice perfusate resulted in reduced or fully impaired hippocampal LTP, whereas aCSF alone permitted LTP (Fig. 1A). In sequential experiments, we found that B24 (Fig. 1B) and B28 (Fig. 1C), when added to the slice perfusate with the Alzheimer's disease brain extract, prevented LTP inhibition. h1C22 appeared protective (Fig. 1A) but did not meet the $\alpha = 0.05$ significance threshold of this study. The clinical trial antibody bapineuzumab, which targets the Aβ N terminus,[22] was also protective (Fig. 1D). These results indicate that both B24 and B28 can inhibit the synaptotoxic effects of naturally occurring, diffusible oAβ, presumably by binding to them. To ensure the protection was specific and not due to experimenter bias, we compared B24 protection versus human IgG1 isotype control with the electrophysiologist blinded to sample identity and found similar protection (Supplementary Fig. 4).

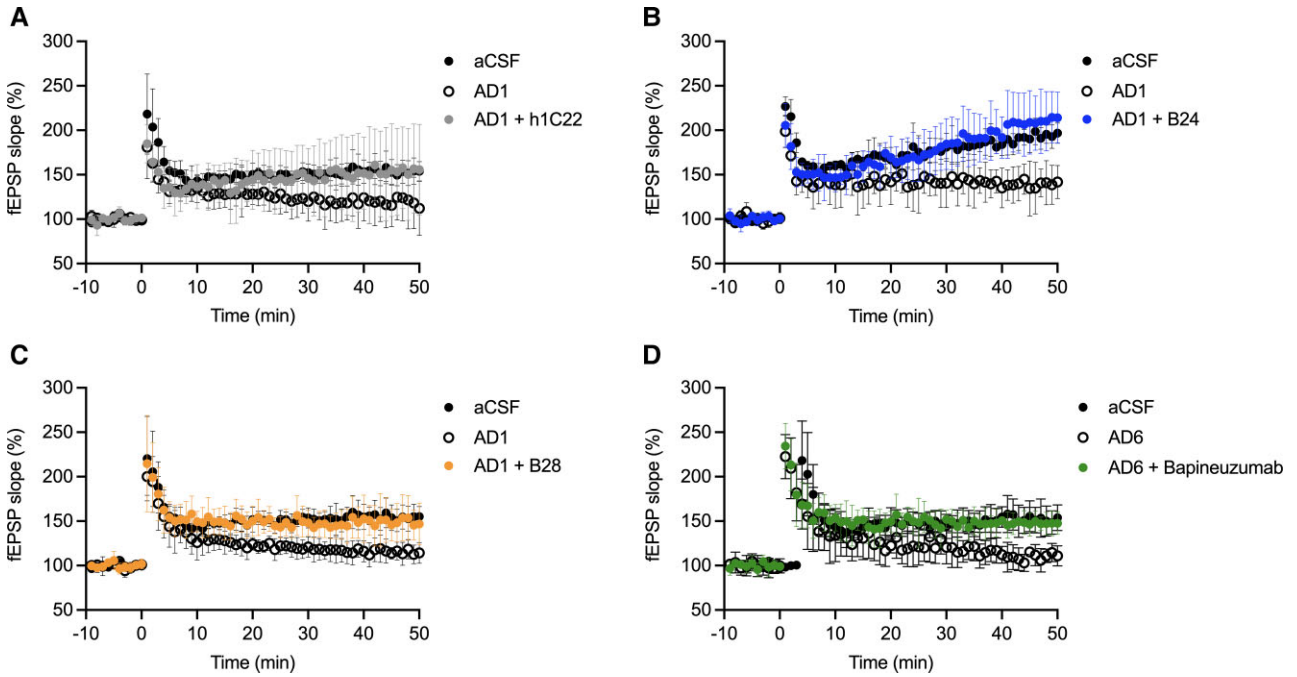

Figure 1 Effect of anti-Aβ antibodies on Alzheimer's disease brain-induced impairment of LTP. Alzheimer's disease (AD) TBS soaking extract impairs mouse hippocampal LTP compared with aCSF alone. Data are presented on the addition of (**A**) h1C22 (**B**) B24, (**C**) B28 and (**D**) bapineuzumab in separate experiments. Error bars reflect mean ± standard deviation. *P*-values were calculated using one-way ANOVA with Tukey's *post hoc* test comparing the means of recorded fEPSP slopes over the last 10 min of the experiment across the three groups within each experiment. *P*-values are as follows: in **A**, $P = 0.15$ for AD versus aCSF; $P = 0.99$ for AD + h1C22 versus aCSF; $P = 0.20$ for AD + h1C22 versus AD. $n = 6$ for aCSF, $n = 6$ for AD, $n = 4$ for AD + h1C22. In **B**, $P = 0.024$ for AD versus aCSF; $P = 0.59$ for AD + B24 versus aCSF; $P = 0.0081$ for AD + B24 versus AD. $n = 4$ for aCSF, $n = 4$ for AD, $n = 3$ for AD + B24. In **C**, $P = 0.0024$ for AD versus aCSF; $P = 0.83$ for AD + B28 versus aCSF; $P = 0.014$ for AD + B28 versus AD. $n = 6$ for aCSF, $n = 5$ for AD, $n = 4$ for AD + B28. In **D**, $P = 0.0002$ for AD versus aCSF; $P = 0.84$ for AD + bapineuzumab versus aCSF; $P = 0.0007$ for AD + bapineuzumab versus AD. $n = 6$ for aCSF, $n = 5$ for AD, $n = 5$ for AD + bapineuzumab.

B24 exhibits unique calcium-dependent binding to natural and synthetic aggregated Aβ

We next determined the ability of B24, B28 and h1C22 to immunoprecipitate naturally occurring, soluble Aβ isolated from Alzheimer's disease brain. Most Aβ in soluble extracts of Alzheimer's disease brain is contained in aggregates that require denaturation with strong chaotropes such as GuHCl to be detected by monomer-preferring ELISAs.[11,13] A minor fraction is detectable without denaturation, and this is presumed to consist mainly of free monomers. We sought to determine which fraction was bound by the respective antibodies and performed immunoprecipitations using protein G magnetic beads, followed by washing and then elution and monomerization of immunoprecipitated aggregates with 5 M GuHCl (Fig. 2A). We found that abundant Aβ could be eluted from B28 and h1C22 but not B24 precipitates (Fig. 2A, *left*), even though B24 provided protection against oAβ-induced impairment of LTP (Fig. 1). By analysing the supernatant after immunoprecipitation, we confirmed that h1C22 and B28 (but not B24) depleted most of the oligomeric Aβ present in GuHCl-denaturable aggregates (Fig. 2A, *middle*). Neither had an effect on the minor Aβ pool that is in a putatively monomeric state in Alzheimer's disease soaking extract, detectable by monomer-preferring ELISAs without GuHCl denaturation (Fig. 2A, *right*). These results imply that h1C22 and B28, as they are with synthetic preparations, are specific for naturally occurring oligomeric Aβ over naturally occurring monomeric Aβ. As expected, the monomer-preferring m266 antibody efficiently immunoprecipitated the natively monomeric fraction (Fig. 2A, *right*) but not the oligomeric fraction (Fig. 2A, *middle*).

The surprising finding that B24 could not immunoprecipitate oAβ from TBS extracts but could protect against LTP impairment led us to hypothesize that a biological substance present in the electrophysiologic experiments may be required for B24 to bind efficiently to Aβ. These initial TBS soaking extracts had been dialysed to remove small molecules such as glutamate that interfere with electrophysiologic experiments. We therefore prepared TBS extracts from the same Alzheimer's disease cortical tissue with and without dialysis and found that B24 could immunoprecipitate oAβ if the extract had not been dialysed (Fig. 2B). Dialysis had no significant effect on immunoprecipitation by h1C22 or B28 (Fig. 2B). Performing the immunoprecipitation on dialysed TBS extract supplemented with complex Neurobasal media (Gibco) restored B24 binding, implying the presence in the latter of a soluble factor sufficient to allow B24 binding to Aβ. Adding components of Neurobasal media one-by-one to a dialysed extract revealed that calcium, but not other components including magnesium, was sufficient to restore immunoprecipitation of Aβ by B24 (Fig. 2C). Notably, calcium is included in the aCSF used for electrophysiology as a prerequisite for synaptic function. Titration revealed that low mM calcium concentrations permitted B24 binding, although not always to the level of B28 and h1C22 (Fig. 2D). Before this point, we had routinely added the chelators EDTA (5 mM) and EGTA (1 mM) to our TBS extraction buffer, serving as protease inhibitors and also slightly enhancing the extraction of Aβ into the soluble pool.[23] Adding ~0.07 mM of the more calcium-specific

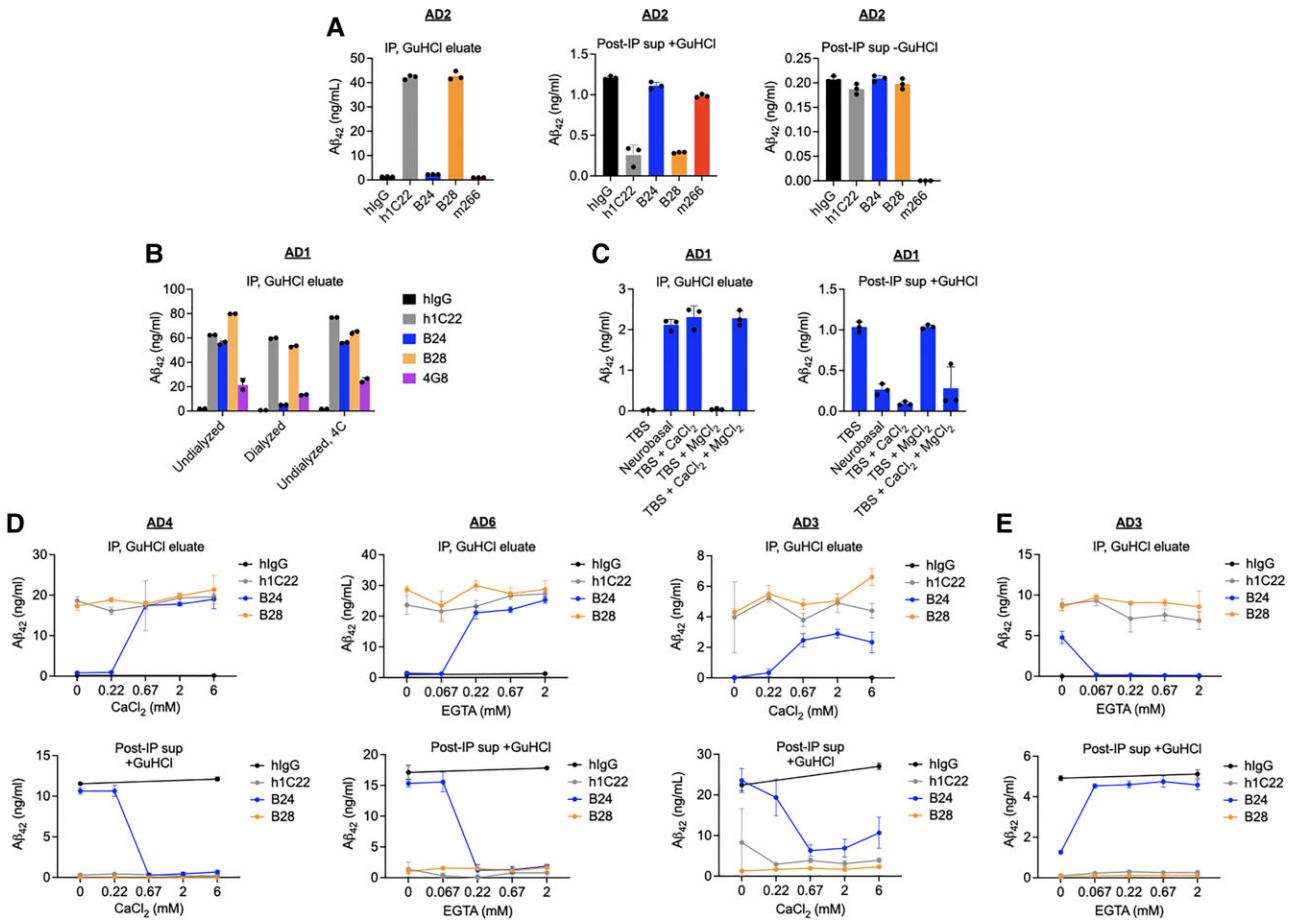

Figure 2 B24 binding to naturally occurring oAβ is strictly calcium-dependent, unlike B28 and h1C22. (**A**) Alzheimer's disease TBS brain-soaking extract prepared in our usual fashion with EGTA and EDTA and then dialysed was diluted in TBS and immunoprecipitated by panel of antibodies with protein G beads. Monomer-preferring Aβ ELISA showed that large amounts of Aβ were pulled down by B28 and h1C22 and released from the beads by GuHCl, but not B24. The quantity of GuHCl-denaturable (i.e. putatively oligomeric) Aβ in the post-immunoprecipitation (IP) supernatant was efficiently depleted by h1C22 and B28 but not B24. There was no effect on natively monomeric Aβ levels measured in the supernatant without GuHCl denaturation. m266 is a control monomer-preferring antibody. hIgG is control non-specific human IgG. (**B**) Alzheimer's disease TBS soaking extract was prepared and divided into three portions. One portion was frozen immediately (Undialysed), one portion dialysed against TBS with two buffer exchanges over 72 h at 4°C (Dialysed) and one portion incubated at 4°C for 72 h (Undialysed, 4C). IP was performed as in **A** and showed that B24 required a dialysable substance for IP, but h1C22 and B28 were unaffected by dialysis. 4G8 is another control antibody with preference for Aβ monomers and some oligomers. (**C**) Dialysed Alzheimer's disease soaking brain extract was diluted in either TBS, Neurobasal media or TBS with supplemental $CaCl_2$ and/or $MgCl_2$ (2 mM) before IP by B24. ELISA of GuHCl bead eluates and post-IP supernatants denatured with GuHCl show that $CaCl_2$ is sufficient for IP by B24. (**D**) IP by multiple antibodies on dialysed TBS soaking extracts from three Alzheimer's disease brains diluted in TBS with $CaCl_2$ titrated as indicated, then GuHCl bead eluates and denatured post-IP supernatants quantified by ELISA. (**E**) IP of Alzheimer's disease TBS soaking extract prepared without chelators or dialysis and increasing concentrations of EGTA, quantifying GuHCl eluate and denatured post-IP supernatant. Error bars represent mean ± SD of three IP events.

EGTA to a previously unchelated and undialysed extract was sufficient to ablate B24 immunoprecipitation of Aβ (Fig. 2E). There was no effect of calcium on B24 binding to the protein G beads, implying that the effect was on B24's binding with Aβ (Supplementary Fig. 6). Together, these results demonstrate that calcium is necessary and sufficient for B24 binding to naturally occurring human oAβ, and we omitted chelators and dialysis from future soaking extracts.

We returned to synthetic Aβ preparations to examine B24 calcium dependence. The initial indirect ELISA screens of hybridoma clones had been performed using antibodies purified in PBS containing calcium. Using Octet biolayer interferometry, we found that B24 (this time purified without calcium) bound synthetic oAβ with equivalent affinity to h1C22 in the presence of 1 mM $CaCl_2$, but that binding was absent without $CaCl_2$ (Fig. 3). Binding of h1C22 and bapineuzumab was unaffected by calcium (Fig. 3). Calculated binding isotherms are listed in Supplementary Table 2.

The Aβ N terminus is required for B24 binding

We hypothesized that the B24 N terminus may be involved in binding to Aβ aggregates because the N terminus is often solvent exposed.[17,18,24,25] To demonstrate this on naturally occurring oAβ, we competed biotinylated B24 with excess non-biotinylated competitor antibodies and precipitated with streptavidin beads. Bapineuzumab, which recognizes a linear epitope in the N terminus,[22] interfered with B24 immunoprecipitation. However, m266, which recognizes the mid-region, did not (Fig. 4A). Using synthetic peptides incubated in the presence of Ca^{2+}, we found that B24, like bapineuzumab, could recognize Aβ deleted of its C-terminal region ($Aβ_{1–28}$) but not Aβ deleted of its N-terminal

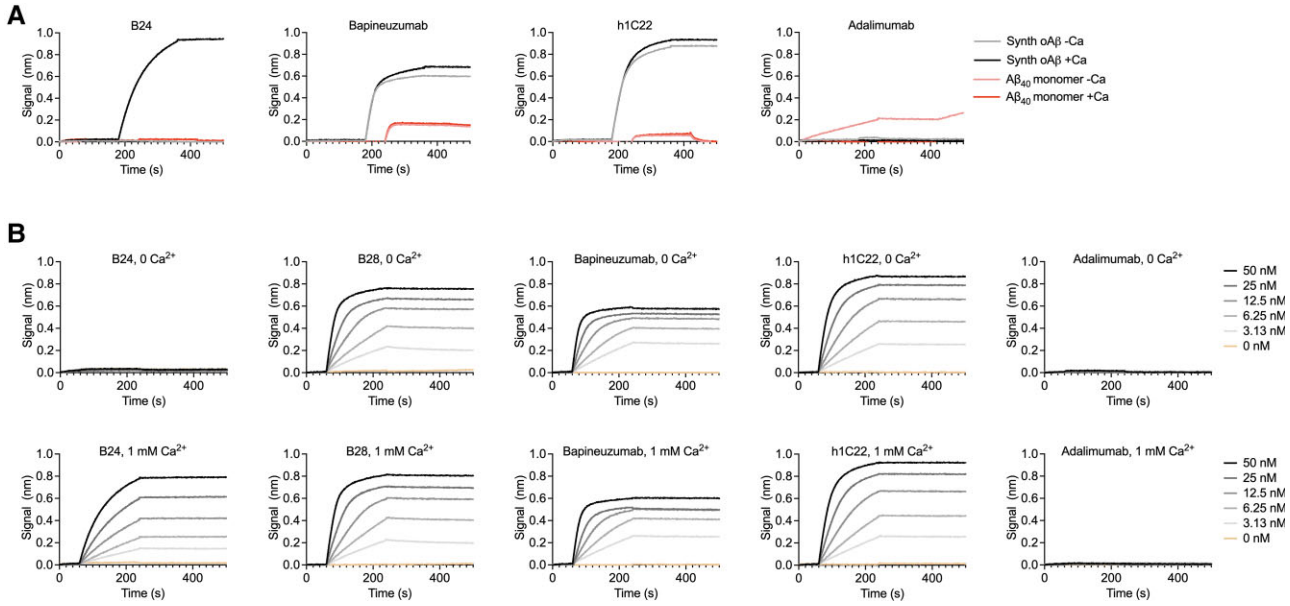

Figure 3 Calcium is necessary for B24 binding to synthetic oAβ. (**A**) Biolayer interferometry curves testing the interaction of antibodies at 100 nM with synthetic oAβ or $Aβ_{40}$ monomer in HEPES-buffered saline with or without 1 mM $CaCl_2$. Bapineuzumab is a positive control antibody with affinity for both Aβ monomers and oligomers. Adalimumab is a negative control antibody against TNFα. Binding isotherms are displayed in Supplementary Table 2. (**B**) A full titration curve against synthetic oAβ shows no substantial effect of Ca^{2+} on any of the antibodies at any concentration except B24.

region ($Aβ_{11–42}$) (Fig. 4B and C). These results indicate that the N terminus is required for forming the B24 epitope.

Calcium affects B24 tertiary structure independent of Aβ

We next sought to determine whether the structure of B24 is affected by calcium using nano-differential scanning fluorimetry. The B24 curves were affected by the addition of 1 mM $CaCl_2$, but B28 curves were not (Supplementary Fig. 5A). Analysing the first derivative of the 350/330 nm fluorescence ratio, we observed an increase from 67 to 68°C in the first melting point (TM1) for B24 by the addition of 1 mM $CaCl_2$, whereas the TM1 of B28 remained at 65°C (Supplementary Fig. 5B). The low TM1 of both antibodies suggests a fragment antigen-binding region (Fab) contribution, but because aggregation was consistent with unfolding for both antibodies, we could not definitively conclude which antibody regions were stabilized by calcium. Nonetheless, these results indicate that calcium can affect the tertiary structure of B24, but not B28, even in the absence of ligand.

B24 labelling of amyloid plaques is calcium-dependent

We next used immunofluorescence histochemistry to examine human Alzheimer's disease tissue staining by B24, B28 and 1C22, using murine-Fc chimeric antibody constructs. In brain tissue from advanced Alzheimer's disease cases, we used cryostat

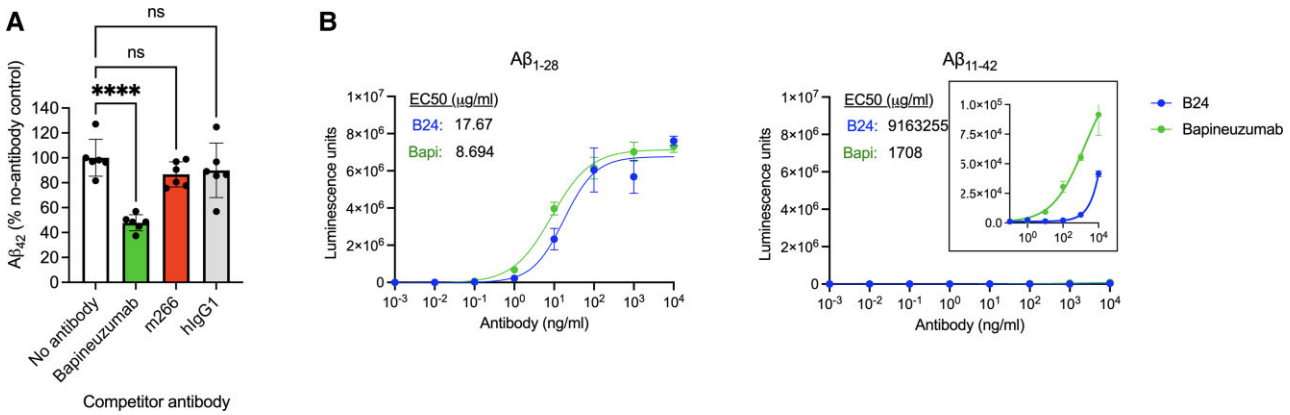

Figure 4 The Aβ N terminus is involved in B24 binding. (**A**) Extract of brain AD7 was immunoprecipitated with streptavidin magnetic beads and biotinylated B24 in the presence of a 100-fold excess of non-biotinylated competitor antibody, then washed in TBS and eluted with GuHCl. ****$P < 0.0001$ by one-way ANOVA with Dunnett's *post hoc* multiple comparisons test. (**B**) Indirect ELISA on synthetic Aβ isoforms aggregated in the presence of Ca^{2+} shows little effect of C-terminal truncation but ablation of binding with N-terminal truncation. Inset on right graph shows faint signal detected at high antibody concentrations.

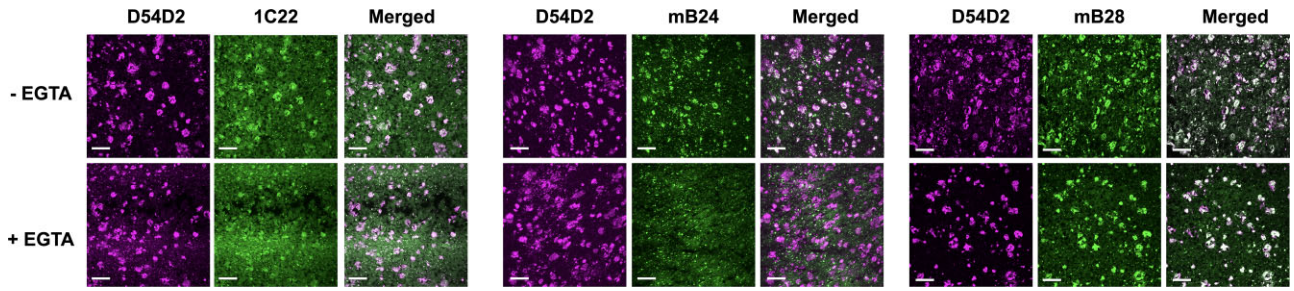

Figure 5 mB24 and mB28 stain some amyloid plaques, but mB24 staining is calcium-dependent. Immunohistofluorescence images of cryostat sections of cortex from case AD4. Aβ N terminus-specific rabbit monoclonal D54D2 was used to identify amyloid plaques (magenta), and costained with the antibody of interest (green), using murine-Fc equivalents of B24 and B28, as well as the original murine 1C22. Sections were prepared without fixation. An additional wash was added with 5 mM EGTA (*bottom row*). mB28 and 1C22 appeared to stain nearly all plaques, whereas mB24 stained a subset. EGTA wash ablated mB24 staining but not mB28 or 1C22. Scale bar = 0.2 mm.

sectioning to obtain frozen sections without fixation, which may affect conformational antibody epitopes. Although the cellular architecture of cryostat sections was largely distorted by ice crystals, amyloid plaques retained their shape and could be identified using the rabbit monoclonal antibody D54D2, a reference Aβ antibody that recognizes a linear epitope at the N terminus. D54D2 consistently stained many plaques (Fig. 5). In unfixed cryostat sections, we found that mB28 stained virtually all plaques, whereas mB24 appeared to stain a subset of plaques. 1C22 labelled all plaques, but more weakly than the other two. Washing the sections in EGTA completely ablated mB24 staining of plaques but not that of 1C22 or mB28, again demonstrating the exquisite calcium dependence of the B24 antibody. Together, these results imply that B24 recognizes a naturally occurring epitope on a subset of plaques in a calcium-dependent manner.

Most human soluble oAβ binds avidly to calcium phosphate mineral

We next sought to determine whether the B24 calcium dependence was solely due to an effect on B24 tertiary structure or whether calcium may also bind avidly to Aβ oligomers as part of a tripartite calcium-oAβ-B24 complex. Notably, the immunofluorescence histochemistry binding buffer was calcium-free, and yet B24 bound to plaques in an EGTA-sensitive manner, implying that its target Aβ antigen was natively calcium-bound. We compared the affinity of Aβ versus tau and α-synuclein to a CHT column by fast protein liquid chromatography. CHT is a mixed-mode chromatography method during which retention on the calcium phosphate resin occurs by calcium-affinity interactions with C-sites and anion exchange interactions with P-sites. Under phosphate-free

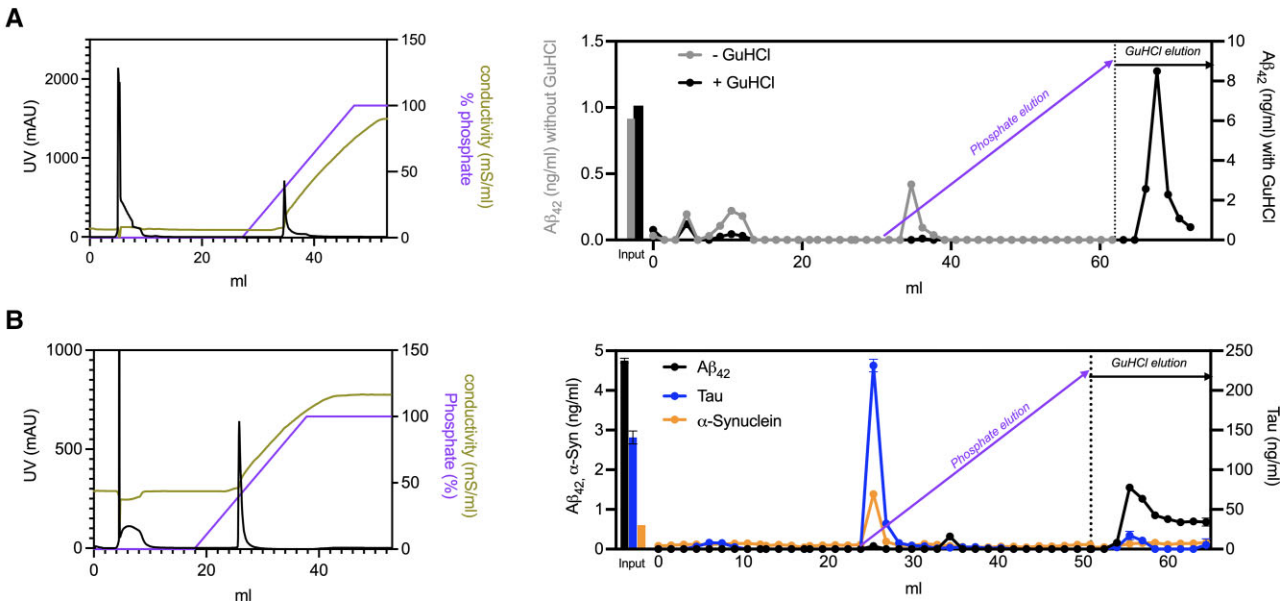

Figure 6 Naturally occurring oAβ binds tightly to CHT. (**A**) Brain AD5 TBS soaking brain extract was chromatographed on a CHT column with binding buffer 50 mM NaCl, 2.5 mM $CaCl_2$, 25 mM HEPES, pH 7.4, conditions under which binding is entirely due to calcium-affinity interactions. Elution occurred through a linear gradient to 1 M KPO_4, pH 7.4. The column was washed in water and then eluted in 6 M GuHCl, 50 mM $NaPO_4$, 50 mM HEPES, pH 7.4. UV chromatogram (*left*) demonstrates that most protein elutes in the void volume or at the start of the phosphate gradient. Sandwich ELISA (*right*) with or without denaturation of each fraction with GuHCl shows that oligomeric Aβ but not natively monomer-preferring ELISA-accessible Aβ requires GuHCl for elution from the CHT column. (**B**) Chromatography was repeated on brain AD4 and raising the NaCl concentration in the binding buffer to 500 mM and the peak gradient KPO_4 concentration to 1.5 M, followed by sandwich ELISA for $Aβ_{42}$, tau and α-synuclein on GuHCl-denatured fractions.

conditions containing calcium, binding to the CHT column is entirely by calcium affinity, and elution takes place via addition of phosphate, which competitively displaces protein carboxyls from hydroxyapatite calcium ions.[26] The UV chromatogram of human soluble Alzheimer's disease brain-soaking extract under these conditions showed that the majority of proteins either did not bind to the CHT column or eluted as a single peak early in the phosphate gradient (Fig. 6A, *left*). ELISA without, versus with, GuHCl revealed that the small amount of natively monomeric ELISA-accessible Aβ present in the input eluted within these two peaks, indicating weak to moderate calcium affinity of natively monomeric Aβ (Fig. 6A, *right*). In contrast, oAβ (i.e. the Aβ requiring GuHCl denaturation for detection by the monomer ELISA) barely eluted in either peak (Fig. 6A, *right*). Instead, release of most soluble Aβ from the CHT column required denaturation with 6 M GuHCl, indicating high affinity to CHT. We repeated this experiment, raising the NaCl concentration from 50 to 500 mM to reduce ion exchange effects at the P-sites and increasing the maximum phosphate concentration in the gradient from 1 to 1.5 M (Fig. 6B). Still, Aβ required GuHCl denaturation to elute off the column (Fig. 6B, *right*). In contrast, both endogenous tau and α-synuclein eluted within the major protein peak early in the phosphate gradient, similar to elution of native Aβ monomer, and no more of either test protein came off with the 6 M GuHCl elution (Fig. 6B, *right*). Thus, the calcium dependence of B24 binding may involve specific and direct interactions of Ca^{2+} ions with Aβ oligomers, in addition to the above-demonstrated effect of Ca^{2+} on B24 conformation *per se*.

In contrast to CHT chromatography, we did not detect any effect of calcium on the size distribution of natural oAβ when measured by non-denaturing SEC (Supplementary Fig. 7B). Incubation of a previously chelated and dialysed Alzheimer's disease TBS soaking extract with versus without calcium, followed by fractionation on a Superdex 75 Increase column, did not alter the retention time of oAβ. As has been observed previously, most oAβ occurred in the void volume.[11–13] In combination with the observation that calcium does not affect the affinity of other oAβ-preferring antibodies we tested (Figs 2 and 3), our results demonstrate that calcium may bind tightly to oAβ but not induce large-scale changes in the size or conformation of the oligomers.

B24 enables affinity enrichment of human oAβ via non-denaturing EGTA elution

Since the calcium dependence appeared reversible and unique to B24, and yet calcium had no major effects on oAβ size, we sought to determine whether B24 could immunoaffinity purify naturally occurring human Aβ oligomers solely by modulating calcium concentration, without the use of detergents or harsh pH changes that could affect the aggregation status of oAβ. We found that B24 immunocapture in the presence of 2 mM $CaCl_2$ followed by washing and elution with 5 mM EGTA yielded roughly one-third of the oAβ that was initially bound by B24 in the soaking extract and could afterwards be released from the beads by GuHCl denaturation (Fig. 7B). Far more Aβ was detectable in the EGTA eluate by monomer-preferring ELISA if it was then denatured in GuHCl (Fig. 7A and B), implying that B24 purified oAβ which maintained its oligomeric state. No Aβ was released by EGTA from B28 immunoprecipates (Fig. 7C). Quantitative bookkeeping revealed a yield of 18.5% and a fold-enrichment of 28.7 compared to the crude extract (input) (Fig. 7D). Like the input, the EGTA-eluted immunopurified material resided in the void volume of a Superdex 200 Increase SEC column (Fig. 7E). To our surprise, examining the B24 EGTA eluate by negative-stain electron microscopy revealed multiple short fibrils ~8 nm in diameter (Fig. 7F–H). This material was labelled with D54D2 and protein A nanogold (Fig. 7I–K), confirming the presence of short Aβ fibrils in the B24-purified material from the Alzheimer's disease brain-soaking extract. As a negative control, we did not observe any fibrils in the EGTA eluate from B28, in keeping with the fact that its binding of Aβ is not Ca^{2+}-sensitive (Fig. 7C).

B24-immunopurified oAβ inhibits synaptic plasticity

Finally, we sought to determine whether the material eluted from B24 by EGTA was synaptotoxic. We found that the yield of total Aβ by EGTA elution from TBS soaking extracts was insufficient to exert an effect on hippocampal LTP, so we used B24-EGTA-purified material from Alzheimer's disease brain-tissue homogenization in TBS. We obtained a higher percentage and total yield of Aβ compared to starting with soaking extracts, and the same 28-fold Aβ enrichment (Fig. 8A). The EGTA-eluted material was still high molecular weight by SEC (Fig. 8B). After desalting to remove the EGTA, addition of the eluate from B24 IP resulted in impairment of LTP, but not so for the EGTA eluate from B28 immunoprecipitation (Fig. 8C and D). These results indicate that B24 binding followed by EGTA elution can isolate bioactive oAβ from Alzheimer's disease cortex, particularly when starting with the soluble fraction from an aqueous homogenate.

Discussion

Here we describe a novel monoclonal antibody, B24, with unique calcium-dependent properties that permits reversible binding of oligomeric but not monomeric Aβ. We observed calcium dependence in solution and in immunolabelling cryostat sections of Alzheimer's disease brain. Calcium-sensitive antibodies derived from animals have been described before, including the M1 anti-FLAG clone[27] and antibodies to protein kinase C[28] and human thrombospondin.[29] In these cases, the epitope itself was sensitive to calcium. The FLAG epitope (DYKDDDDK) possesses many negatively charged acidic residues that coordinate Ca^{2+} ions required for M1 binding. The M2 anti-FLAG clone binds the same epitope in a non-Ca^{2+}-dependent manner.

We suspect a similar phenomenon may occur with oAβ, in which a Ca^{2+}-binding epitope can be formed by certain folds of the peptide. Accordingly, we found that most naturally occurring soluble oAβ binds avidly to Ca^{2+} in the form of hydroxyapatite. Endogenous Aβ has been identified on hydroxyapatite deposits in the retina of patients with macular degeneration,[30] and calcium has been shown to accelerate the aggregation of synthetic Aβ into oAβ and fibrils *in vitro*.[31] Recent data suggest structural possibilities for how oAβ might bind Ca^{2+}. In one cryo-electron microscopy structure of natural Aβ aggregates (from meningeal fibrils), a previously unidentified fold brings into proximity carboxyl side-chains of Asp1 and Glu3 with carboxyl side-chains of Glu22 and Asp23 in a manner that may coordinate a Ca^{2+} ion.[17] This fold was not observed in *in vitro*-prepared synthetic amyloid fibrils.[32] A more recent cryoEM structure of brain-derived Aβ filaments from parenchymal plaques found a metal coordination site at Glu22 and Asp23,[18] but the N terminus was not resolved in those structures. Consistent with these observations, Itkin *et al.*[33] showed that addition of calcium to synthetic wild-type $Aβ_{40}$ caused it to aggregate similarly to calcium-free $Aβ_{40}$ possessing the familial Alzheimer's disease E22G mutation. Altogether, we

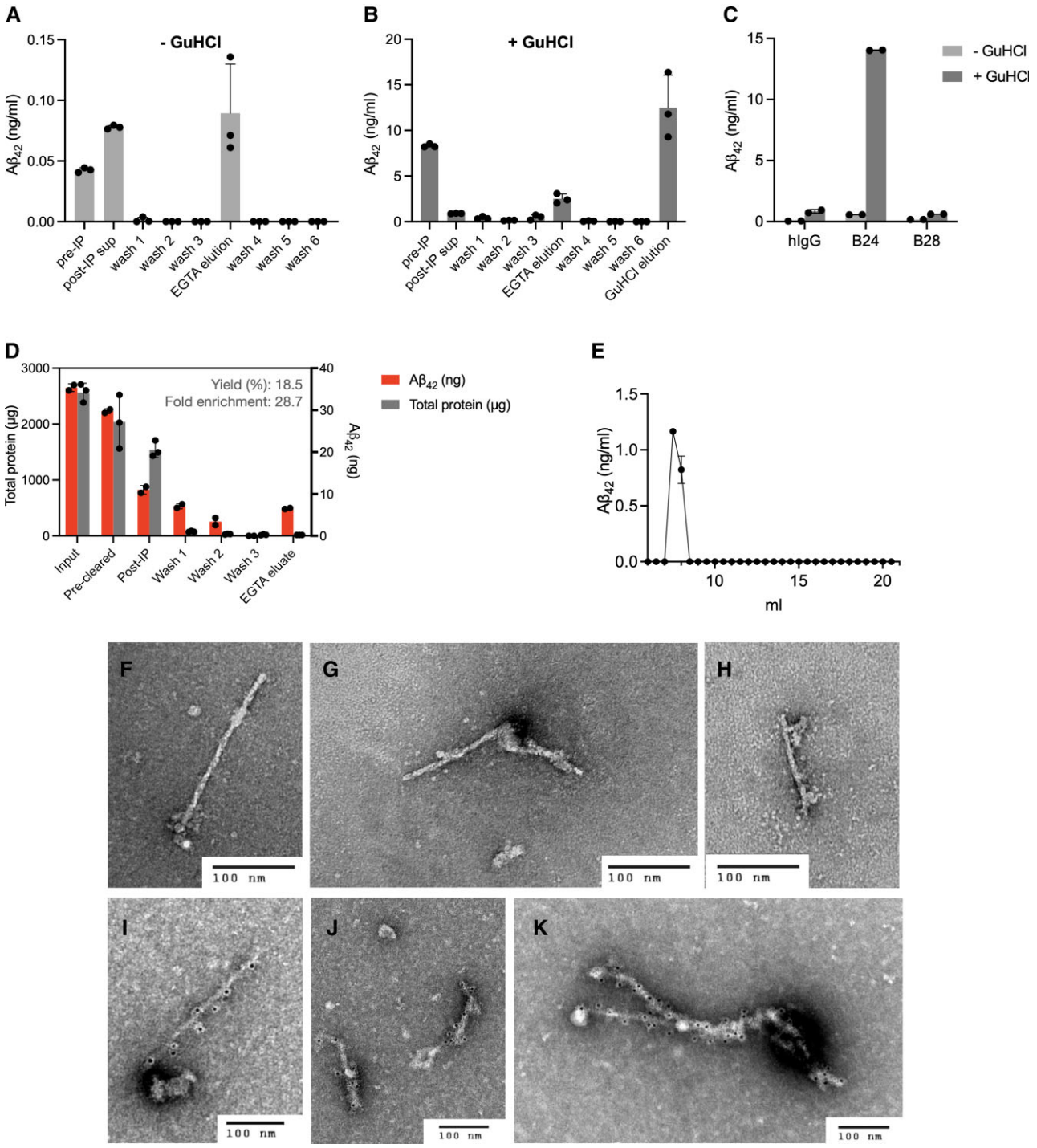

Figure 7 B24 allows non-denaturing isolation of naturally occurring oAβ-derived fibrils. (**A** and **B**) One millilitre of brain AD3 TBS soaking extract was diluted four-fold in TBS + 2 mM $CaCl_2$ and 'pre-cleared' with protein A magnetic beads in the absence of antibody. Extract was then mixed with 0.5 ml of fresh washed protein A magnetic beads (Pierce) and 200 µg B24, incubated 4°C overnight, washed five times in TBS without $CaCl_2$, then eluted in 0.5 ml of TBS + 5 mM EGTA overnight at 4°C. Samples were retained and evaluated by sandwich ELISA without (**A**) or with (**B**) denaturation by GuHCl. Results indicate that B24 caused the release of a small amount of natively monomeric (ELISA-accessible) Aβ, far less than the total Aβ immunoprecipitated detectable after denaturation. (**C**) Repeating the procedure in **A** and **B** using hIgG and B28 on brain AD4 showed that EGTA cannot elute Aβ from these antibodies. (**D**) Quantitative bookkeeping of total protein and total GuHCl-denatured $Aβ_{42}$ from a soaking extract of brain AD7. (**E**) SEC of EGTA eluate from **D** on a Superdex 200 Increase column showing that the material elutes in the SEC void volume. (**F**–**H**) Negative staining electron microscopy of EGTA-eluted B24-purified material demonstrated elongated helical fibrils 8–10 nm in diameter. (**I**–**K**) Immunogold labelling with D54D2 (rabbit anti-Aβ N-terminal antibody) labelled each fibril with many gold particles. Electron microscopy results representative of two Alzheimer's disease brains.

propose that B24, Ca^{2+} and certain naturally occurring Aβ aggregates can form a tripartite complex via an Aβ fold involving the N terminus and E22 and D23. Our data suggest that it is unlikely for Ca^{2+} to induce a large-scale conformational change in Aβ oligomers or fibrils once they have formed, because there was no change in binding of two other conformation-sensitive antibodies

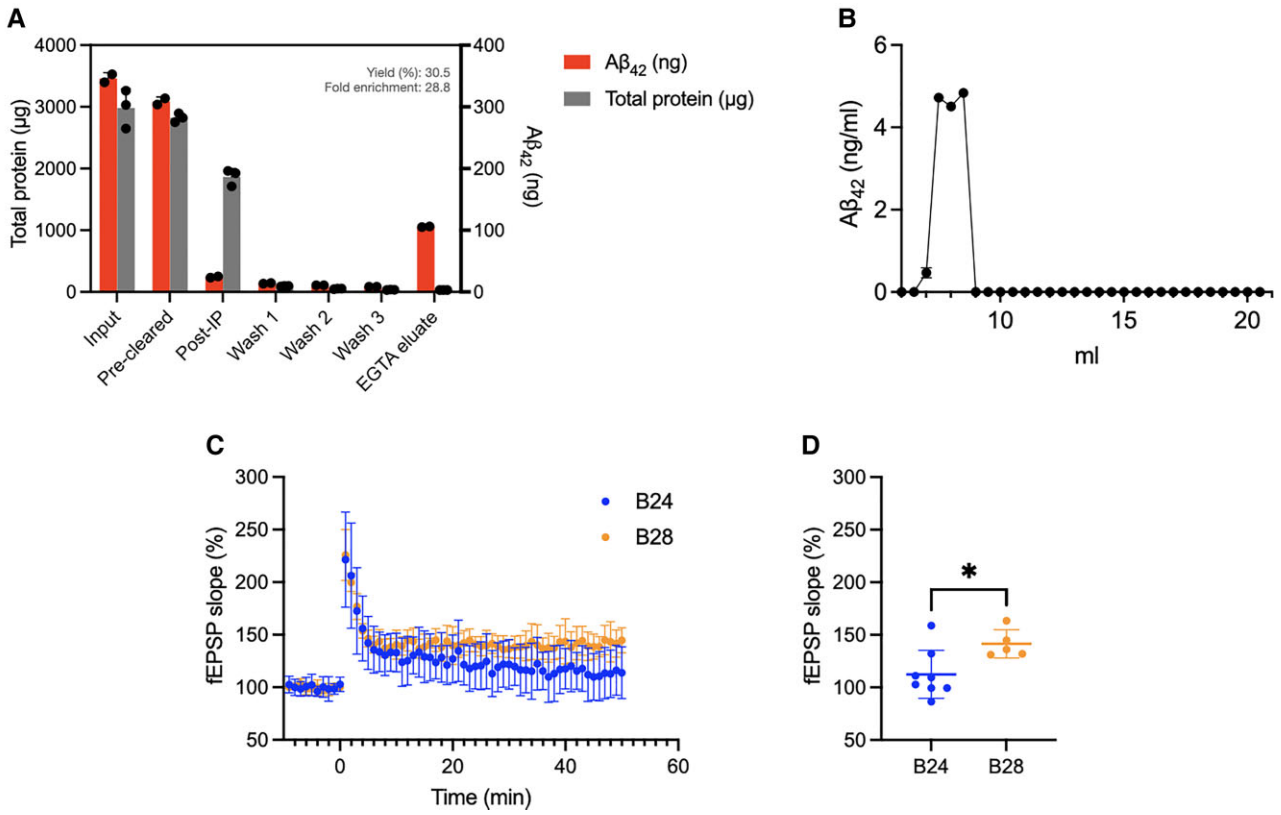

Figure 8 Aβ immunopurification by B24 from Alzheimer's disease brain homogenate results in higher yield and bioactivity. (**A**) Quantitative bookkeeping of total protein and total GuHCl-denatured $Aβ_{42}$ from a homogenate extract of brain AD7. (**B**) SEC of EGTA eluate from (**A**) on a Superdex 200 Increase column showing that the material is within the SEC void volume. (**C**) Effect of EGTA eluate (after desalting) from B24 or B28 immunoprecipitation on LTP. (**D**) Comparison of mean of last 10 min of recording for each slice between B24 eluate and B28. $n = 8$ slices for B24, $n = 5$ slices for B28. Error bars represent mean ± SD. *$P < 0.05$ by unpaired Student's *t*-test.

(h1C22; B28) in solution or on Alzheimer's disease brain sections, nor did altering the calcium concentration noticeably affect the size distribution of soluble oAβ by SEC. B24 bound only a subset of the plaques that were bound by a conventional N-terminal Aβ antibody (D54D2) or other oAβ-specific antibodies; one explanation is that there may be a diversity of oAβ folds, only some of which bind Ca^{2+}.

Taking advantage of the reversible calcium dependence of B24, we were surprised to find that immunoaffinity enrichment of oAβ was associated with short amyloid fibrils observed by electron microscopy. Several explanations are possible and will be the subject of future study. Fibrils could be present in the initial soluble soaking extract but may not pellet during the ultracentrifugation step due to their association with buoyant substances such as lipids. Alternatively, the fibrils may not be present initially but arise from non-fibrillar soluble seeds on their concentration by the antibody on the surface of beads. It is currently unknown what proportion of the total oAβ isolated by B24 is fibrillar versus present in smaller oligomeric forms that are not visible by electron microscopy. It is also unknown whether the fibrils we observe are similar in structure or composition to those present in amyloid plaques, and whether it is fibrillar or non-fibrillar forms of oAβ from the soluble brain extracts that are the principal synaptotoxin. Reactivity with anti-fibril antibody OC has previously led to the hypothesis that 'fibrillar oligomers' may exist in soluble extracts of Alzheimer's disease brain tissue and correlate with dementia, corroborating our finding.[34] Esparza *et al.*[35] reported immunoaffinity purification of oAβ from human brain-soluble extracts but did not observe fibrils, seeing only smaller, amorphous aggregates. Reasons could include different centrifugation speeds and rotors, different antibodies for immunoprecipitation, their blocking all tubes and tips in BSA, and their use of ammonium hydroxide (pH 10.5) for elution, which may have induced some disassembly as opposed to the TBS + EGTA that we used.

Our study has important limitations. Beyond the data present in Fig. 4, we could not define the epitope of B24 at the level of individual residues, because of the likely three-dimensional nature of the conformational epitope and the differences between naturally occurring oAβ and the synthetic oligomers to which it must be compared. Furthermore, we restricted the current study to a limited number of Alzheimer's disease brains used to identify the unique calcium dependence of B24 binding, but a future larger study could more precisely determine what proportion of natural oAβ binds B24 and binds Ca^{2+}. Finally, we have not yet defined whether the unique properties of B24 render it a promising immunotherapeutic compared to existing oAβ-directed antibodies such as lecanemab.[36] We plan to test B24 as an oAβ-neutralizing and -clearing antibody in mouse models and determine whether Ca^{2+}-bound oAβ is a particularly neurotoxic subspecies compared to the total oAβ pool.

In summary, we describe a novel calcium-sensitive oAβ-selective antibody, B24, and its ability to immunopurify bioactive Aβ oligomers from soluble extracts of human brain under non-denaturing conditions, at least some of which display fibrillar character. The key significance of these results is that they hold promise for further

structural and biochemical studies of naturally occurring, purified brain oAβ, which has thus far been elusive.

Acknowledgements

We thank Dominic Walsh and Tim Weeden for early discussions and preparation of synthetic aggregates. We thank Tara Travaline for assistance with assay development. We thank Mel Feany for tissue allocation.

Funding

This work was funded by NIH grants R01AG006173 (D.J.S.) and P01AG015379 (D.J.S.), the Davis Alzheimer Prevention Program (D.J.S.) and a collaborative grant from Sanofi.

Competing interests

D.J.S. is a director and consultant of Prothena Biosciences. S.K., T.S., M.B., D.R. and L.P. are employees of Sanofi. All other authors declare no competing interests.

Supplementary material

Supplementary material is available at *Brain* online.

References

1. Lue LF, Kuo YM, Roher AE, *et al*. Soluble amyloid beta peptide concentration as a predictor of synaptic change in Alzheimer's disease. *Am J Pathol*. 1999;155(3):853–862.
2. Esparza TJ, Zhao H, Cirrito JR, *et al*. Amyloid-β oligomerization in Alzheimer dementia versus high-pathology controls. *Ann Neurol*. 2013;73(1):104–119.
3. McLean CA, Cherny RA, Fraser FW, *et al*. Soluble pool of Aβ amyloid as a determinant of severity of neurodegeneration in Alzheimer's disease. *Ann Neurol*. 1999;46(6):860–866.
4. Jin M, Shepardson N, Yang T, Chen G, Walsh D, Selkoe DJ. Soluble amyloid beta-protein dimers isolated from Alzheimer cortex directly induce Tau hyperphosphorylation and neuritic degeneration. *Proc Natl Acad Sci U S A*. 2011;108(14):5819–5824.
5. Zott B, Simon MM, Hong W, *et al*. A vicious cycle of β amyloid–dependent neuronal hyperactivation. *Science*. 2019;365(6453):559–565.
6. Li S, Jin M, Koeglsperger T, Shepardson NE, Shankar GM, Selkoe DJ. Soluble Aβ oligomers inhibit long-term potentiation through a mechanism involving excessive activation of extrasynaptic NR2B-containing NMDA receptors. *J Neurosci*. 2011;31(18):6627–6638.
7. Shankar GM, Li S, Mehta TH, *et al*. Amyloid-β protein dimers isolated directly from Alzheimer's brains impair synaptic plasticity and memory. *Nat Med*. 2008;14(8):837–842.
8. Nilsberth C, Westlind-Danielsson A, Eckman CB, *et al*. The "Arctic" APP mutation (E693G) causes Alzheimer's disease by enhanced Aβ protofibril formation. *Nat Neurosci*. 2001;4(9):887–893.
9. Tucker S, Möller C, Tegerstedt K, *et al*. The murine version of BAN2401 (mAb158) selectively reduces Amyloid-β protofibrils in brain and cerebrospinal fluid of tg-ArcSwe mice. *J Alzheimers Dis*. 2015;43:575–588.
10. Englund H, Sehlin D, Johansson A-S, *et al*. Sensitive ELISA detection of amyloid-β protofibrils in biological samples. *J Neurochem*. 2007;103(1):334–345.
11. McDonald JM, O'Malley TT, Liu W, *et al*. The aqueous phase of Alzheimer's disease brain contains assemblies built from ∼4 and ∼7 kDa Aβ species. *Alzheimers Dement*. 2015;11(11):1286–1305.
12. Yang T, Li S, Xu H, Walsh DM, Selkoe DJ. Large soluble oligomers of Amyloid β-protein from Alzheimer brain are far less neuroactive than the smaller oligomers to which they dissociate. *J Neurosci*. 2017;37(1):152–163.
13. Hong W, Wang Z, Liu W, *et al*. Diffusible, highly bioactive oligomers represent a critical minority of soluble Aβ in Alzheimer's disease brain. *Acta Neuropathol*. 2018;136(1):19–40.
14. Benilova I, Karran E, De Strooper B. The toxic Aβ oligomer and Alzheimer's disease: an emperor in need of clothes. *Nat Neurosci*. 2012;15(3):349–357.
15. Wildburger NC, Esparza TJ, LeDuc RD, *et al*. Diversity of Amyloid-beta proteoforms in the Alzheimer's disease brain. *Sci Rep*. 2017;7(1):9520.
16. Brinkmalm G, Hong W, Wang Z, *et al*. Identification of neurotoxic cross-linked amyloid-β dimers in the Alzheimer's brain. *Brain*. 2019;142(5):1441–1457.
17. Kollmer M, Close W, Funk L, *et al*. Cryo-EM structure and polymorphism of Aβ amyloid fibrils purified from Alzheimer's brain tissue. *Nat Commun*. 2019;10(1):4760.
18. Yang Y, Arseni D, Zhang W, *et al*. Cryo-EM structures of Amyloid-β 42 filaments from human brain.*Science*. 2022;375:167–172.
19. Jin M, O'Nuallain B, Hong W, *et al*. An in vitro paradigm to assess potential anti-Aβ antibodies for Alzheimer's disease. *Nat Commun*. 2018;9(1):2676.
20. Yang T, O'Malley TT, Kanmert D, *et al*. A highly sensitive novel immunoassay specifically detects low levels of soluble Aβ oligomers in human cerebrospinal fluid. *Alzheimers Res Ther*. 2015;7(1):14.
21. Mably AJ, Liu W, Mc Donald JM, *et al*. Anti-Aβ antibodies incapable of reducing cerebral Aβ oligomers fail to attenuate spatial reference memory deficits in J20 mice. *Neurobiol Dis*. 2015;82:372–384.
22. Feinberg H, Saldanha JW, Diep L, *et al*. Crystal structure reveals conservation of amyloid-β conformation recognized by 3D6 following humanization to bapineuzumab. *Alzheimers Res Ther*. 2014;6(3):31.
23. Cherny RA, Legg JT, McLean CA, *et al*. Aqueous dissolution of Alzheimer's disease Aβ Amyloid deposits by biometal depletion. *J Biol Chem*. 1999;274(33):23223–23228.
24. Qiang W, Yau WM, Lu JX, Collinge J, Tycko R. Structural variation in amyloid-β fibrils from Alzheimer's disease clinical subtypes. *Nature*. 2017;541(7636):217–221.
25. Lu JX, Qiang W, Yau WM, Schwieters CD, Meredith SC, Tycko R. Molecular structure of β-Amyloid fibrils in Alzheimer's disease brain tissue. *Cell*. 2013;154(6):1257–1268.
26. Gagnon P, Cheung CW, Yazaki PJ. Reverse calcium affinity purification of fab with calcium derivatized hydroxyapatite. *J Immunol Methods*. 2009;342(1–2):115–118.
27. Hopp TP, Gallis B, Prickett KS. Metal-binding properties of a calcium-dependent monoclonal antibody. *Mol Immunol*. 1996;33(7):601–608.
28. Ohlin A-K, Stenflo J. Calcium-dependent interaction between the epidermal growth factor precursor-like region of human protein C and a monoclonal antibody. *J Biol Chem*. 1987;262(28):13798–13804.
29. Dixit VM, Galvin NJ, O'Rourke KM, Frazier WA. Monoclonal antibodies that recognize calcium-dependent structures of human thrombospondin: characterization and mapping of their epitopes. *J Biol Chem*. 1986;261(4):1962–1968.

30. Thompson RB, Reffatto V, Bundy JG, *et al*. Identification of hydroxyapatite spherules provides new insight into subretinal pigment epithelial deposit formation in the aging eye. *Proc Natl Acad Sci U S A*. 2015;112:1565–1570.
31. Isaacs AM, Senn DB, Yuan M, Shine JP, Yankner BA. Acceleration of Amyloid β-Peptide aggregation by physiological concentrations of calcium. *J Biol Chem*. 2006;281(38):27916–27923.
32. Gremer L, Schölzel D, Schenk C, *et al*. Fibril structure of amyloid-β(1-42) by cryo-electron microscopy. *Science*. 2017; 358(6359):116–119.
33. Itkin A, Dupres V, Dufrêne YF, Bechinger B, Ruysschaert JM, Raussens V. Calcium ions promote formation of amyloid β-peptide (1-40) oligomers causally implicated in neuronal toxicity of Alzheimer's disease. *PLoS One*. 2011;6(3):e18250.
34. Tomic JL, Pensalfini A, Head E, Glabe CG. Soluble fibrillar oligomer levels are elevated in Alzheimer's disease brain and correlate with cognitive dysfunction. *Neurobiol Dis*. 2009;35(3):352–358.
35. Esparza TJ, Wildburger NC, Jiang H, *et al*. Soluble Amyloid-beta aggregates from human Alzheimer's disease brains. *Sci Rep*. 2016;6:38187.
36. Swanson CJ, Zhang Y, Dhadda S, *et al*. A randomized, double-blind, phase 2b proof-of-concept clinical trial in early Alzheimer's disease with lecanemab, an anti-Aβ protofibril antibody. *Alzheimers Res Ther*. 2021;13(1):80.